

INTERNATIONAL WORKSHOP ON FAST CHERENKOV DETECTORS - PHOTON DETECTION,
DIRC DESIGN AND DAQ
NOVEMBER 11–13, 2015, GIESSEN, GERMANY

High-performance DIRC detector for the future Electron Ion Collider experiment

G. Kalicy,^{a,1} L. Allison,^a T. Cao,^b R. Dzhygadlo,^c T. Horn,^d C. Hyde,^a Y. Ilieva,^b
P. Nadel-Turonski,^e K. Park,^a K. Peters,^c C. Schwarz,^c J. Schwiening,^c J. Stevens,^e W. Xi^e
and C. Zorn^e on behalf of PID Consortium for an integrated program for Particle
Identification (PID) at a future Electron-Ion Collider

^aOld Dominion University,
Norfolk, U.S.A.

^bUniversity of South Carolina,
Columbia, U.S.A.

^cGSI Helmholtzzentrum für Schwerionenforschung GmbH,
Darmstadt, Germany

^dThe Catholic University of America,
Washington, U.S.A.

^eThomas Jefferson National Accelerator Facility,
Newport News, U.S.A.

E-mail: gkalicy@jlab.org

ABSTRACT: A radially-compact subsystem providing particle identification (e/π , π/K , K/p) over a wide momentum range is an essential requirement for the central detector of an Electron-Ion Collider (EIC). With a radial size of only a few cm, a detector based on Detection of Internally Reflected Cherenkov light (DIRC) principle is a very attractive solution. The R&D undertaken by the EIC PID consortium achieved the goal of showing feasibility of a high-performance DIRC that would extend the momentum coverage well beyond state-of-the-art allowing 3σ separation of π/K up to 6 GeV/c, e/K up to 1.8 GeV/c and p/K up to 10 GeV/c. A key component to reach such a performance is a special 3-layer spherical compound lens. This article describes the status of the design and R&D for the DIRC at EIC detector, with a focus on the detailed Monte Carlo simulation results for the high-performance DIRC.

KEYWORDS: Cherenkov and transition radiation; Cherenkov detectors; Photon detectors for UV, visible and IR photons (vacuum)

¹Corresponding author.

Contents

1	Introduction	1
2	DIRC detector performance	3
3	Compound 3-layer lens	4
4	DIRC for EIC design	5
5	Performance in Monte Carlo simulations	6
6	Experimental validation	9
7	Summary	10

1 Introduction

The Electron Ion Collider (EIC) is planned to be the next large project for nuclear physics research in the U.S. It will be the world's first collider with polarized electron and light ion beams, and capable of heavier, unpolarized ion beams up to uranium. The current design of the Jefferson Lab full-acceptance detector is shown in figure 1. A central solenoid provides a magnetic field. Particle Identification (PID) detectors include electro-magnetic calorimeters, a fast time-of-flight detector (TOF), and three Cherenkov detectors: modular aerogel and dual radiator Ring Imaging Cherenkov detectors (RICH) and a DIRC detector. Selection and arrangement of the sub-detectors were optimized to detect and identify the complete final state of a nuclear reaction, including all partonic and nuclear fragments. Excellent hadronic PID in the central detector over a large range of solid angle and particle momenta is essential for studying the current jets, in particular through exclusive and semi-inclusive processes, which allow for imaging of the 3D structure of the nucleon. It is also important for heavy-flavor. The physics objectives of the future EIC experiments are discussed in detail in [1].

One of the key challenges for charged hadron PID of the EIC detector is the separation of pions from kaons. The use of three different technologies based on Cherenkov radiation assures complete momentum and angular coverage. On average, hadrons produced in asymmetric ep collisions and detected on the electron side have momenta up to the electron beam energy, those scattered on the hadron side up to the ion beam energy. In the EIC the beam energies will be on the order of 10 GeV for electrons and 100 GeV for pions. The highest energy region is in the hadron part and there a dual radiator RICH covering momentum up to 50 GeV is a good choice, the aerogel RICH is envisioned to cover momentum up to 10 GeV on the electron unit side. In the barrel region the lowest energies have to be covered by a system that will be surrounded by an electromagnetic calorimeter that constrains radiation length and has to be able to operate in the fringe field of the

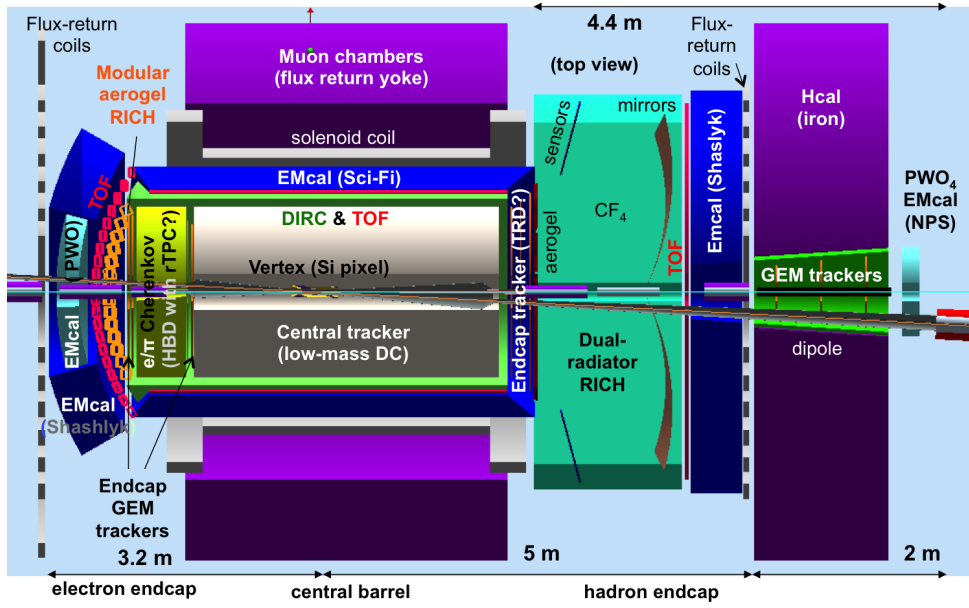


Figure 1. Top view of current layout of the full acceptance JLab EIC detector with all subsystems. The detector is divided into the three regions, a middle barrel region, an electron side around a left endcap, and an ion side around a right endcap.

solenoid, a non-uniform magnetic field of a magnitude of 3 T or higher. A great solution that meets these requirements is a detector based on the DIRC principle, moreover, a high-resolution DIRC covering momenta up to 5–6 GeV with a separation power of at least 3 standard deviations would be a perfect match.

The BaBar DIRC was the first, and up to now still is the only DIRC detector used in a large high-energy physics experiment. For more than 8 years this robust and stable system was successfully operated at SLAC [2] for hadronic PID and inspired several experiments to include DIRC detectors in their design or upgrade plans. One of those is the PANDA experiment at the FAIR facility [3], now in the final phase of R&D, which selected a Focusing DIRC (FDIRC) counter for the barrel region of the target spectrometer. The performance reached by the BaBar DIRC meets the PANDA requirements. However, because of the different environment and geometry in PANDA, mostly space limitations, the design of the DIRC detector required important modifications. The whole system was made more compact and a smaller expansion volume was placed inside the solenoid magnet. This compact design required focusing optics as well as small-pixel photosensors and fast electronics to maintain the resolution and make it work in the PANDA environment. The geometrical constraints for the DIRC readout planned for EIC are similar to the PANDA Barrel DIRC. Therefore, the EIC DIRC design is inspired by the design of the PANDA Barrel DIRC detector and many synergies exist in the R&D processes of both projects. The primary goal of developing a high-performance DIRC is to have a compact device that can satisfy the PID requirements of the EIC.

This article describes the current design of the high-performance DIRC system envisioned for the EIC detector. The general aspects of DIRC detectors along with a discussion of required and achievable performance are discussed in section 2. The key component of the design of the high-

performance DIRC detector is a special 3-layer lens described in section 3, followed by section 4 discussing the design of full the detector. Performance studied in Geant4 simulations are presented in section 5 and experimental tests which are currently in progress are discussed in section 6.

2 DIRC detector performance

A DIRC detector, like other Cherenkov counters, uses the fact that a charged particle traversing a medium faster than the light in that medium generates Cherenkov photons on a cone with the half opening angle θ_C defined as $\cos \theta_C = 1/n(\lambda)\beta$, where $\beta = v/c$, v is the particle velocity, and $n(\lambda)$ is the index of refraction of the medium (which, for a dispersive medium, is a function of the wavelength (λ) of the Cherenkov photons). In the case of a DIRC detector, as shown in figure 2a, solid bars made from synthetic fused silica are utilized both as radiators and light guides. For $\beta \approx 1$ of the traversing particle some of the photons will always be caught inside the radiator due to total internal reflection, and will propagate towards either end of the radiator. A rectangular cross section and parallel, highly polish surfaces conserve the magnitude of the Cherenkov angle during reflections. Photons that originally propagate away from the readout volume will be reflected back by a mirror attached to the end of the radiator. Photons that exit the radiator into the expansion region are imaged in three dimensions by an array of sensors: x , y , and arrival time. The measured position and propagation time of each photon are combined with information from the tracking system to reconstruct the track Cherenkov angle and to determine the corresponding PID likelihoods.

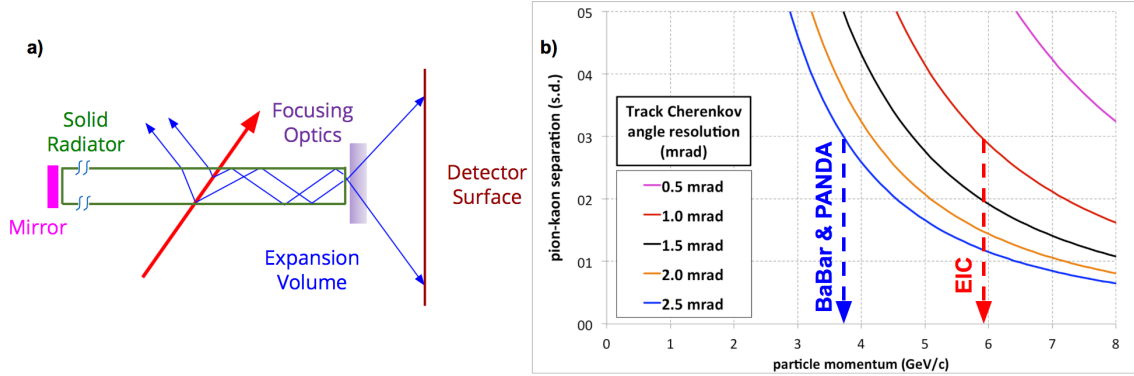


Figure 2. a) Working principle of a DIRC detector. b) π/K separation in standard deviations as a function of momentum. The color of the lines indicates the Cherenkov angle resolution per track, which contains contributions from the DIRC detector and the tracking system.

The PID performance of a DIRC detector is primarily driven by three parameters that can be folded into the track Cherenkov angle resolution σ_C , defined as $\sigma_C^2 = \sigma_{C,\gamma}^2/N_\gamma + \sigma_{\text{track}}^2$, where N_γ is the number of detected Cherenkov photons from each particle, $\sigma_{C,\gamma}$ is the Cherenkov angle resolution per photon, and σ_{track} is the uncertainty of the particle direction in the DIRC, dependent mainly on the resolution of the tracking system.

Figure 2b shows how an increased momentum range for π/K separation translates into better track Cherenkov angle resolution. In an EIC, the pion background for kaons varies with reaction channel and kinematics, but is typically about 3:1. The usual 3σ criterion thus seems relevant.

Achieving 3σ separation using radiator bars of fused silica would require a Cherenkov angle resolution per particle of 1.3 mrad at 5 GeV/c and 1.0 mrad at 6 GeV/c. Achieving this resolution assumes that the central tracker will be able to provide an angular resolution at the sub-mrad level or that the effect of the tracking resolution on the Cherenkov angle measurement can be mitigated in software.

The blue dashed arrow in figure 2b shows that $\sigma_C = 2.5$ mrad is sufficient to operate a DIRC up to 3.8 GeV/c and to reach both the BaBar and the PANDA PID goals. However, the EIC physics program requires π/K separation up to 6 GeV/c and, as shown by the red dashed arrow, in that case the track Cherenkov angle resolution has to be on the level of 1 mrad. Such an upgrade to the system resolution forced revisiting all the separate contributions to photon yield and the single photon Cherenkov angle resolution ($\sigma_{C,\gamma}$). $\sigma_{C,\gamma}$ is a sum in quadrature of contributions from the pixel size ($\sigma_{C,\text{det}}$), bar size $\sigma_{C,\text{bar}}$, bar imperfections ($\sigma_{C,\text{trans}}$), and the chromatic dispersion ($\sigma_{C,\text{chrom}}$):

$$\sigma_{C,\gamma}^2 = \sigma_{C,\text{det}}^2 + \sigma_{C,\text{bar}}^2 + \sigma_{C,\text{trans}}^2 + \sigma_{C,\text{chrom}}^2.$$

As suggested by the above equation, there are five ways to improve the Cherenkov angle resolution. The focusing optic can be used to reduce the size of the image from the DIRC bar. To better resolve the image the pixel size of the readout sensors can be decreased. There are various possibilities to improve the photon yield. It is possible to reduce the chromatic effect from the uncertainty in the photon production angle due to the dispersion $n(\lambda)$ through precise timing (100 ps or better) or by using wavelength filters (also an intrinsic feature of most radiation hard glasses). Last but not least, one can reduce the size of the correlated term, the uncertainty of the track direction. The DIRC R&D for the EIC has to address all of these aspects and consider the potential improvement versus cost. For example, tightening the already very tough constraints on the optical finish used by BaBar and PANDA bars would bring very little improvement with a huge increase to the cost. On the other hand, the influence of the bar size, $\sigma_{C,\text{bar}}$, on the resolution can be mitigated by a focusing system and it will be discussed in next section in more detail.

3 Compound 3-layer lens

The concept of DIRC using focusing mirrors was first studied in the FDIRC R&D program [4]. The PANDA Barrel DIRC introduced a solution with focusing lenses. At first a simple plano-convex lens, made of fused silica and an air gap between the lens and expansion volume, was studied. It was able to produce a well-focused image of the Cherenkov pattern in the central region of the ring image. However, due to the refractive index jump at the air gap many photons are reflected back due to the Fresnel reflection, especially for steep angles between the photon and the surface normal vector. For particles traversing a bar at angles close to perpendicular the photon yield, therefore, drops to close to zero. As a solution, a special 2-layer lens was designed and built to eliminate the air gap by using transitions between fused silica and a higher-refractive index material. However, such a 2-layer lens, as well as a standard single-layer lens, unavoidably produces a parabolic-shaped focal plane described by the Petzval field curvature [5]. This effect is shown in figure 3a in a Geant4 simulation of the DIRC setup with a 2-layer spherical lens made of fused silica and lanthanum

crown glass (NLaK33, refractive index $n = 1.786$ for $\lambda = 380$ nm). The red parabolic line shows the shape of the focal plane as a function of the angle of the photons going through the lens. For photons perpendicular to the lens, the focal point is 40 cm, while for at the steepest angles the focal distance shortens to 5 cm. The parabolic shape of focal plane was confirmed experimentally and can be found in [6]. For a prism-shaped expansion volume this large variation of focal lengths causes part of the ring segment to be out of focus. Although this large aberration would have been acceptable for the PANDA Barrel DIRC the lens design had to be improved to reach the resolution of a high-performance DIRC. To solve this issue for the EIC DIRC a special 3-layers lens was designed in Zemax optical software [7] and in Geant4 simulation with an NLaK33 layer between two layers of synthetic fused silica. It has two different radii of curvature to create defocussing and focusing surfaces to shape the focal plane. The resulting improvement is shown for a Geant4 simulation of the 3-layer spherical lens in figure 3b. The properly selected combination of a focusing and a defocussing surface produces a flat focal plane even for photon polar angles of 40° or more.

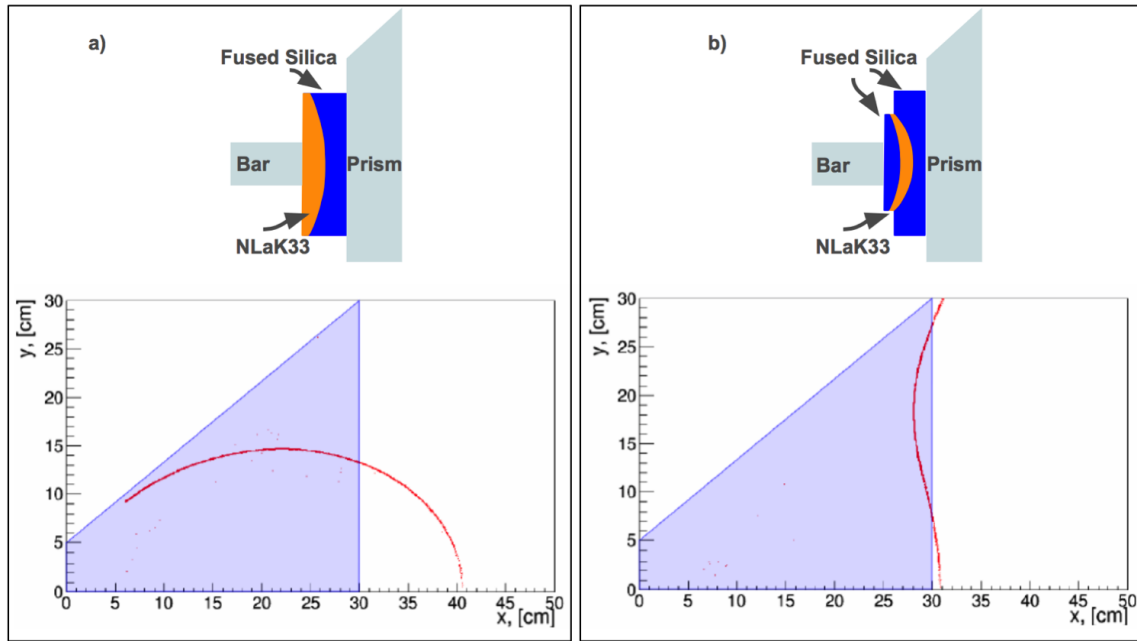


Figure 3. Drawings of bar/lens/prism combination with a 2-layer lens (a) and the 3-layer lens (b). The figures below each lens drawing show the simulated shape of the corresponding focal plane overlaid on the prism shape.

4 DIRC for EIC design

The baseline design, implemented in a Geant4 simulation, is shown in figure 4. The radiators are synthetic fused silica bars, each 4200 mm long, with a cross-section of $17 \text{ mm} \times 35.4 \text{ mm}$ divided into 16 modules, called bar boxes. In each box eleven bars are placed side-by-side and separated by a small air gap. The 16 bar boxes are arranged in a barrel with a radius of 1m around the beam line. Mirrors are attached to one end of each bar. On the readout end, where photons exit the bar, a special 3-layer lens, that will be described further, is attached to each bar. The other side

of the 3-layer lens is coupled directly to a prism that serves as an expansion volume. A zoom into the readout end of the bar box, showing details of the lens and prism section is shown on a right side of figure 4. The prism is made of fused silica, has a 38° opening angle, and has dimensions of $284.3 \text{ mm} \times 390 \text{ mm} \times 300 \text{ mm}$. The detector plane of each prism is covered by 27,690 $2 \text{ mm} \times 2 \text{ mm}$ pixels giving a total of about 443,040 channels to record the location and arrival time of the Cherenkov photons.

Geant4 simulations assuming different pixel sizes were performed to study possible improvement of $\sigma_{C,\text{det}}$. Reducing the pixel size is not technically challenging for the manufacturers, but it will increase the channel density and cost. Figure 5a shows the single photon Cherenkov angle resolution (SPR) as a function of the pixel size for four angles of the incoming charged particle track. A pixel size of 2–3 mm would be a good choice for the high-performance DIRC design, which is less than half the size of the standard square Planacon Micro-Channel Plate Photomultiplier Tubes (MCP-PMTs) [8]. The exact sensors used in this simulation are not yet commercially available so the quantum efficiency of the pixels is taken from data sheets of Photonis MCP-PMTs as they are closest to the considered sensors for the final DIRC for EIC detector. The R&D program focused on improving existing sensors to fulfill all the DIRC for EIC requirements is summarized in [10].

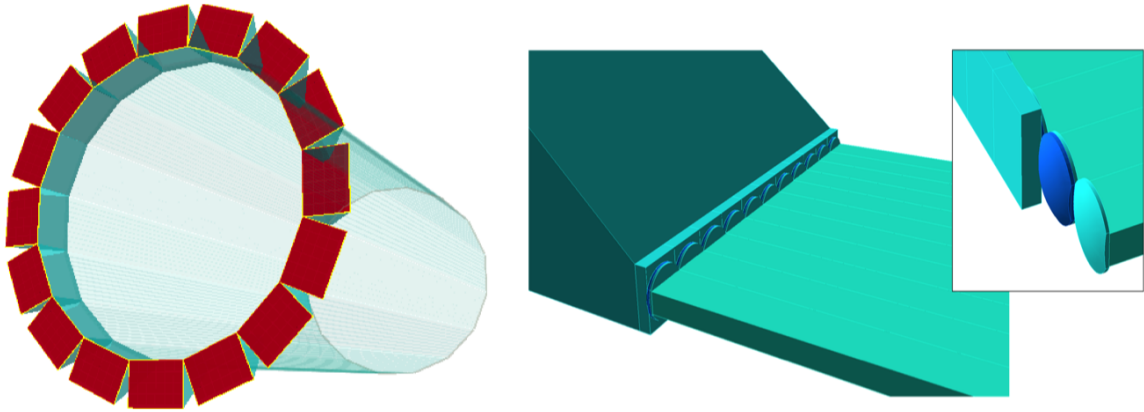


Figure 4. A Geant4 implementation of the tentative geometry of a lens-based, high-performance DIRC for the EIC with narrow bars and a solid fused silica prism. Shown on the right is a zoom of the prism expansion volume, a row of spherical 3-layer lenses, and the radiator bars. The insert shows the individual lenses and layers of the spherical lens system.

5 Performance in Monte Carlo simulations

The performance of the DIRC detector and initial designs are evaluated through Monte Carlo Geant4 simulation with a special set of variables that can be measured later in the test beam experiment. These variables are the single photon Cherenkov angle resolution and the photon yield, which are also easily related to the performance reached in BaBar and required for EIC.

The photon yield is obtained by counting all hits within a certain time window in each selected event. The reconstruction method of the Cherenkov angle is based on the geometrical reconstruction, based on the method used for the BaBar DIRC. The geometric reconstruction algorithm is used to quantify the Cherenkov angle resolution. In Geant4 simulation a monochromatic photon source is

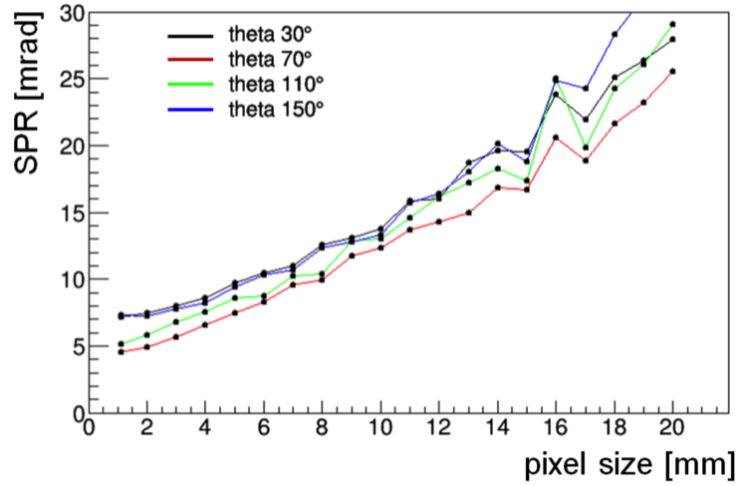


Figure 5. Influence of the pixel size on the single-photon Cherenkov angle resolution for selected track polar angles (θ) from Geant4 simulation with the current DIRC for EIC design.

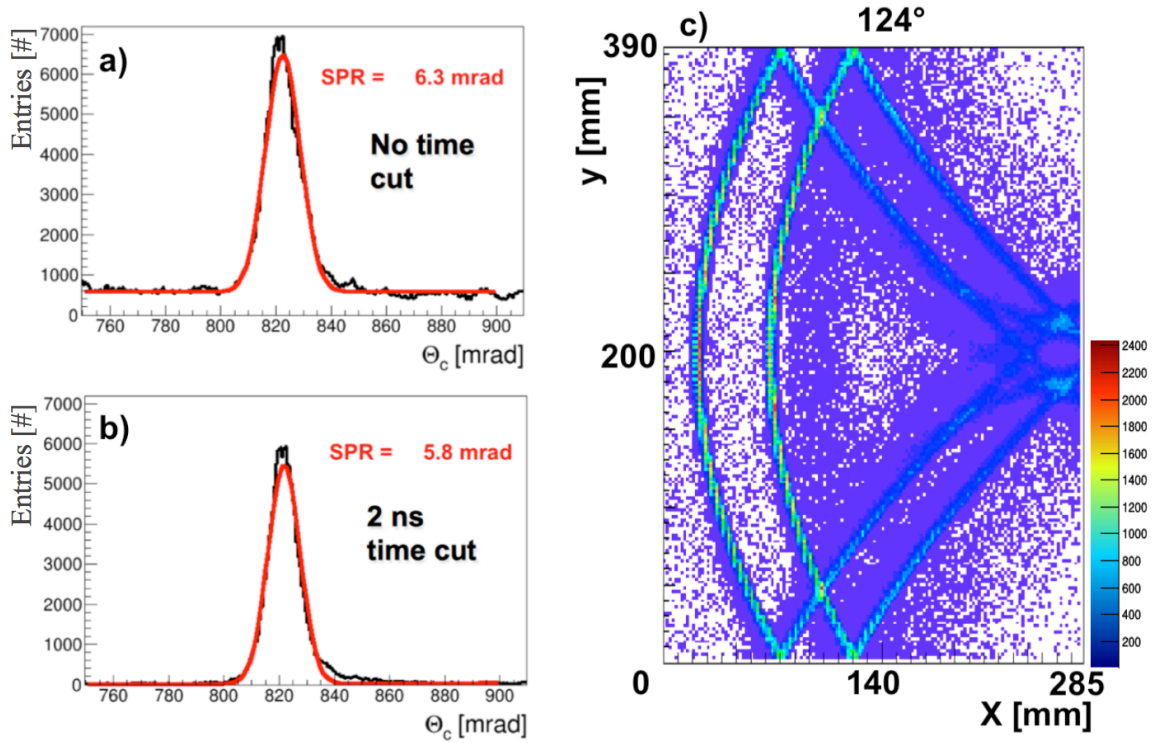


Figure 6. Reconstructed single-photon Cherenkov angle for simulated data using Geant4. 6 GeV/c pions are entering the high-performance DIRC setup at a 124° angle, without time cut (a), and with 2-ns time cut (b). Corresponding occupancy plot on array of sensors with 2 mm pixels (c).

placed in the bar close to the readout end and photons are emitted over the entire phase space. After propagation of the photons through the lens and the prism expansion volume, a look-up table is created associating each sensor pixel with the center of the bar end surface with a specific unit wave

vector \hat{k} . In addition, the time of propagation for each photon path is saved. A separate look-up table is created for photons with each combination of reflections in the prism. Photons can reach a pixel directly, or with some combination of reflections off the sides, top, and bottom of the prism. In the reconstruction process a Cherenkov angle θ_C is calculated from:

$$\cos \theta_C = \hat{k} \times p$$

where p is the beam unit vector in the bar coordinate system for each detected photon. The value of θ_C is histogrammed, including the 8-fold ambiguity from all possible reflections off the surfaces of the DIRC bar and around 30-50 all possible paths in the prism. Reconstructed false photon propagation paths generate combinatorial background around the main peak in the θ_C distribution, but a clear peak remains around the correct angle. The single-photon Cherenkov angle resolution is obtained by fitting a Gaussian plus polynomial to the accumulated θ_C histogram as shown in figure 6a for 100k 6 GeV/c pions transversing bar at 124° . Figure 6b shows that part of the false photon paths can be rejected by a time cut, suppressing some of the combinatorial background. This time cut is performed on the distribution of the difference between the measured arrival time of the photons and the expected propagation time for photons of the average wavelength of 380 nm obtained from the look-up table. An occupancy plot for the simulated data used in this reconstruction is shown in figure 6c.

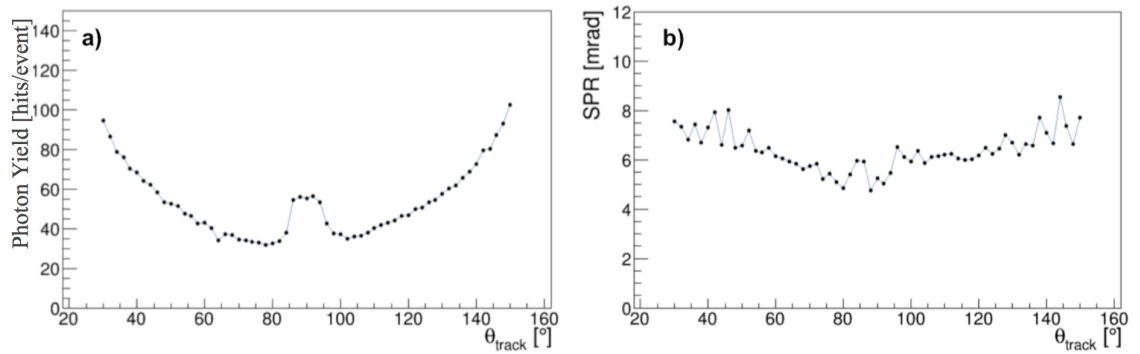


Figure 7. Photon yield (a) and single-photon Cherenkov angle resolution (SPR) (b) as a function of particle track polar angle from Geant4 simulation of 6 GeV/c pions and the lens-based high-performance DIRC, assuming a sensor packing fraction of 100%.

The average number of photoelectrons per track (photon yield) as a function of the particle track polar angle is shown in figure 7a. It is worth noting the large yields around 90° where regular lenses with an air gap would provide almost zero yield. The reconstructed single-photon Cherenkov angle resolution, as a function of the particle track polar angle is shown in figure 7b. The resulting resolution per track is shown in figure 8b for different angular resolution of the central tracker, which measures the angle at which the incoming particle enters the radiator bar. The simulation shows how critical the tracker is for achieving optimal PID performance. Assuming that this could approach 0.5 mrad, a high-performance EIC DIRC should be able to reach a θ_C resolution of 1 mrad, or a 3σ π/K separation up to 6 GeV/c, and an e/π separation up to 1.8 GeV/c.

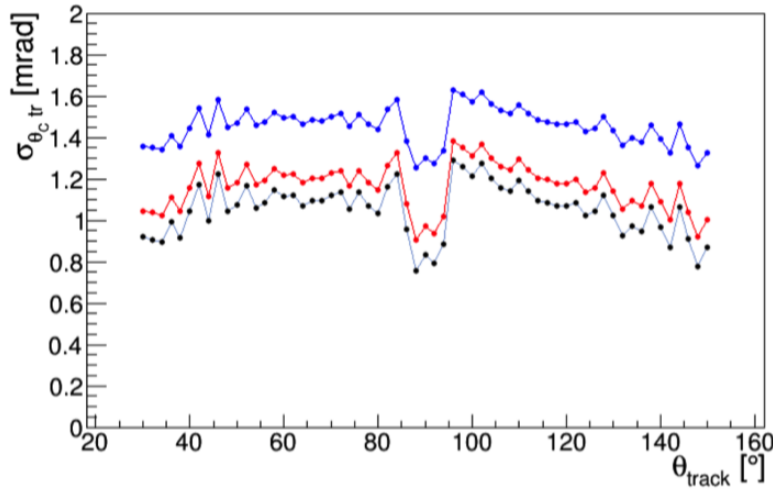


Figure 8. Geant4 results for the track Cherenkov angle resolution assuming three different angular resolutions for the central tracker: 0 mrad (black), 0.5 mrad (red), and 1 mrad (blue).

6 Experimental validation

Experimental validation for the properties of the 3-layer lens is crucial for the DIRC in the EIC R&D program. Pictures of the prototype lens are shown in figure 9a. Not all of the other components of the high-performance DIRC baseline design are available (such as sensors with small pixels, etc.). However, the validation of the simulation package, used to optimize the design and to determine the performance, can be done by simulating key DIRC for EIC components in a geometry corresponding to the currently available detector prototypes, and by comparing to test beam data. Here, the most important item is the special 3-layer lens. The PANDA Barrel DIRC group provided an opportunity to evaluate the performance of the 3-layer lens in a real particle beam experiment at CERN in 2015. The modular design of the PANDA Barrel DIRC prototype allowed for easy exchange of several components between measurements to test their impact on the prototype performance. The EIC-DIRC simulation package was used for designing the prototype, monitoring the measurements, and analyzing the data. Several different focusing options were tested during the 2015 test beam campaign at the T9 zone at the CERN PS. While the detailed analysis of the beam data is still ongoing, initial results can be found in ref. [11].

The focal planes of the standard spherical lens and a prototype 2-layer lens were studied in Geant4 simulation and validated in experiment. To measure the shape of the focal plane of the 3-layer spherical lens, a special setup was designed and built at the Old Dominion University laser lab. The schematic of the setup is shown in figure 9b. The lens will be placed on a rotating stage and rotated through two parallel laser beams. The intersection point of the two laser beams determines the focal length. The lens will be placed inside a $30 \times 40 \times 60 \text{ mm}^3$ glass container filled with mineral oil (with a refractive index very close to fused silica) to simulate the focusing behavior for the situation without the air gap. The 3-layer lens is placed in a special 3D-printed holder that makes it possible to map out the focal plane in all three dimensions, which will be particularly important for comparing spherical and cylindrical lens designs.

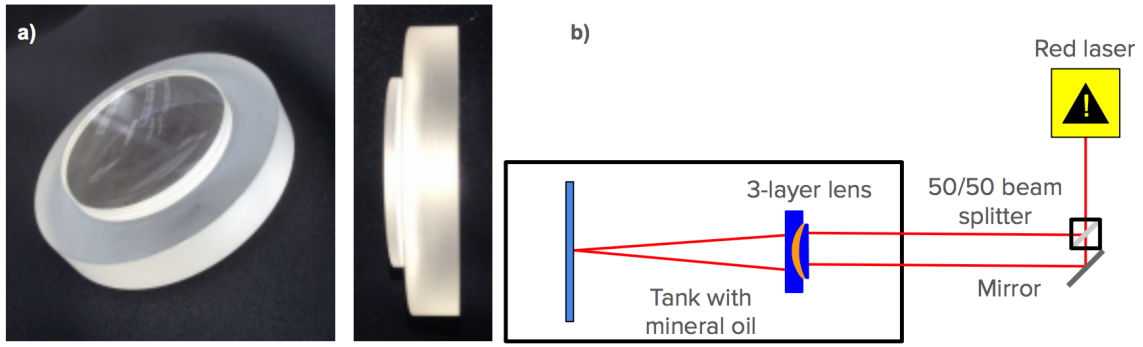


Figure 9. a) Photo of the 3-layer lens prototype. The lens diameter is 50 mm. b) Schematic diagram of the optical setup to map out the focal plane of the 3-layer lens as a function of rotation angle of the lens.

The determination of the radiation hardness of materials is an important study in EIC R&D. Synthetic fused silica, which is used for most of the optical components in all DIRC systems, was already extensively tested in the BaBar and PANDA experiments and proved to be radiation hard. However, in the 3-layer lens the middle layer is made of a high-refractive-index glass, NLak33, which has yet to be tested for radiation hardness. The irradiation will be performed at Catholic University of America in an X-ray setup with energies up to 160 keV in 20 steps, each time delivering a dose of 0.5 krad. Between each step the transmission properties of the lens and a pure NLak33 sample will be measured in a setup with a reproducibility of 0.2% to quantify the impact of the radiation.

Meanwhile, possible alternatives to NLak33 for the next iteration of the 3-layer lens prototype are being investigated. However, optical glasses with high refractive index, especially if they are radiation-hard, typically cut off UV photons at around 400 nm. Lead fluoride (PbF_2) has a high refractive index ($n = 1.77$), is radiation hard, and has a cut off at 300 nm. With this material a flat focal plane at a required distance can be achieved. Prototyping a lens from PbF_2 is in progress and it will show if this material is mechanically usable for lens production.

7 Summary

The initial goal of the DIRC R&D undertaken as part of the Generic R&D for an EIC program was to demonstrate the feasibility of building a high-performance DIRC that would extend the momentum coverage by up to 50% beyond state-of-the-art. Through Geant4 simulations this goal was achieved by developing the lens-based high-performance DIRC. It uses an approach with BaBar-like boxes with narrow bars, each coupled to an advanced spherical 3-layer lens and a compact prism expansion volume made of fused silica. A new type of spherical 3-layer lens with a high index of refraction (no air gap between lens and expansion volume) was designed and produced. It provides a good photon yield, excellent single-photon resolution, and resolves aberrations present in regular focusing lenses. The 3-layer lens is a key component of the high-performance DIRC which, in combination with a high-quality tracking system, is capable of reaching a track Cherenkov resolution of 1 mrad in simulation. Such a performance will allow 3σ separation of e/K up to 1.8 GeV/c, π/K up to 6 GeV/c, and p/K up to 10 GeV/c. Benefiting from very significant synergies with the PANDA

Barrel DIRC development, were able to validate key aspects of the performance of the optics in test beams at CERN. Data was taken and analysis is ongoing.

Acknowledgments

This work was supported in part by BNL under eRD4 and in part by the U.S. National Science Foundation under grant PHY-125782.

References

- [1] A. Accardi et al., *Electron Ion Collider: The Next QCD Frontier - Understanding the glue that binds us all*, [JLAB-PHY-12-1652](#) [[arXiv:1212.1701](#)].
- [2] BABAR DIRC collaboration, I. Adam et al., *The DIRC particle identification system for the BaBar experiment*, *Nucl. Instrum. Meth. A* **538** (2005) 281.
- [3] PANDA CHERENKOV collaboration, G. Kalicy et al., *Status of the PANDA Barrel DIRC*, [2014 JINST 9 C05060](#).
- [4] SUPERB collaboration, *SuperB Technical Design Report. Technical Report*, [INFN-13-01-PI](#), LAL-13-01, SLAC-R-1003, 2013 [[arXiv:1306.5655](#)].
- [5] E. Hecht, *Optics*, 4th edition, Addison-Wesley (2002).
- [6] G. Kalicy, *Development and Test of a Prototype for the PANDA Barrel DIRC Detector at FAIR*, PhD. thesis, Goethe University in Frankfurt (2015).
- [7] Radiant Zemax, 22908 NE Alder Crest Drive, WA 98053 U.S.A., <http://www.radiantzemax.com>.
- [8] PHOTONIS, 660 Main Street, Sturbridge, MA 01518, U.S.A., <https://www.photonis.com/uploads/datasheet/pd/PLANACON-8x8-datasheet.pdf>.
- [9] J. Benitez, D.W.G.S. Leith, G. Mazaheri, B.N. Ratcliff, J. Schwiening, J. Vávra et al., *Status of the Fast Focusing DIRC (fDIRC)*, *Nucl. Instrum. Meth. A* **595** (2008) 104.
- [10] Y. Ilieva et al., *MCP-PMT Studies at the High-B Test Facility at Jefferson Lab*, in *Proceedings of the International Workshop on Fast Cherenkov Detectors - Photon detection, DIRC design and DAQ*, November 11–13, 2015, Giessen, Germany.
- [11] R. Dzhygadlo et al., *The PANDA Barrel DIRC*, [2016 JINST 11 C05013](#).